Magnetic properties of the site-diluted spin-1 Ising superlattice

N. El Aouad, B. Laaboudi, M. Kerouad, and M. Saber
Département de Physique, Faculté des Sciences, Université Moulay Ismail, B.P. 4010, Meknès, Morocco

F. Dujardin and B. Stébé
Laboratoire de Théorie de la Matière Condensée, Université de Metz–Institut de Physique et d'Electronique, 1, Boulevard Arago, 57078 Metz Cedex 3, France

(Received 6 July 2000; published 16 January 2001)

The critical behavior of a diluted spin-1 Ising superlattice is examined using the effective-field theory with a probability distribution technique that accounts for the self-spin correlation functions. The critical temperature of the system is studied as a function of the exchange interactions in each material, the concentration of magnetic atoms, and the thickness of the constituents in a unit cell. A critical value of the interface exchange interaction above which the interface magnetism appears is found. We calculated also some magnetic properties of a diluted spin-1 Ising superlattice such as the layer longitudinal magnetizations and quadrupolar moments. It is shown that the properties of the diluted system are different from those of the corresponding pure system.

DOI: 10.1103/PhysRevB.63.054436 PACS number(s): 75.70.Ak, 75.70.Cn

I. INTRODUCTION

Magnetic layered structures and superlattices have attracted significant attention recently because of a wide array of fascinating properties. The study of a magnetic superlattice that consists of two or more ferromagnets with different bulk properties has been motivated by the idea that the properties of the superlattice can be significantly different from those of their constituents. A detailed review of the properties of magnetic multilayers and superlattices has appeared.[1]

With the advance of modern vacuum science, in particular the epitaxial growth technique, it is possible to grow very thin magnetic films, of predetermined thicknesses, even of a few monolayers. Superlattice structures composed of two different ferromagnetic layers have already been artificially fabricated. Ferromagnetic ordering in some of these monolayers has been reported and the critical properties of such systems have been studied, either experimentally[2–5] or theoretically.[6–15] For a periodic multilayer system formed from two ferromagnetic materials, Fishman, Schwable, and Schwenk[8] have discussed its statics and dynamics within the framework of the Ginzburg-Landau formulation. They have computed the transition temperature and spin-wave spectra. The Landau formalism of Camley and Tilley has been applied to calculate the critical temperature in this system.[10] For a more complicated superlattice with an arbitrary number of different layers in an elementary unit, Barnaś[11] has derived some general dispersion equations for the bulk and surface magnetic polaritons. These equations are then applied to magnetostatic modes and retarded wave propagation in the Voigt geometry.[12]

On the other hand, there is a class of magnetic substances that are well approximated by simple or site-diluted Ising systems.[16–19] Notable examples are Cs_3Cl_5, $DyPo_4$, $Fe_pMg_{1-p}Cl_2$, $Fe_pCo_{1-p}Cl_2$, and $Cd_{1-p}Mn_pTe$. Each of them may be a promising candidate for being prepared in the form of a superlattice and the critical measurements. From the experimental point of view it is possible to synthesize the multilayered systems in which each layer thickness is regulated on the atomic scale.[20] Therefore it is possible to design the structure of the sample so as to fit it to the study of a specific fundamental physics problem. Examples of such experimental studies dealing with the interface and dealing with the surface magnetic order problem when the bulk of the sample is paramagnetic were reported by Shinjo *et al.*[20] and Rau *et al.*,[21] respectively. For the site-diluted systems, the magnetic atoms on the same lattice sites are randomly replaced by nonmagnetic atoms. Generally speaking, the magnetic properties of the diluted magnetic systems may be obviously different from those of the corresponding pure systems. It has been known that a lot of new physical phenomena can appear in these magnetic systems. Kaneyoshi, Tamura, and Sarmento[22] investigated a semi-infinite system with surface dilution by means of the effective-field theory with correlations. Qiang Hong[23,24] and Benyoussef, Boccara, and Saber[25] studied the diluted semi-infinite system using the mean-field theory and renormalization-group method, respectively. Ferchmin and Maciejewski[26] have studied a diluted Ising film and predicted that the surface magnetic phase can appear when the concentration of magnetic atoms on the surface is high enough.

Saber *et al.*[27] have studied the phase diagrams of the site diluted spin-$\frac{1}{2}$ Ising superlattice using the effective-field theory and they have shown that the properties of the diluted system are different from those of the corresponding pure system.

All the studies mentioned above are concerned with Ising systems with $S=\frac{1}{2}$. For $S=1$, the properties of bulk Ising magnetic systems,[28] semi-infinite magnetic systems,[29] and Ising magnetic thin films[30–33] were discussed. However, it is difficult to find studies of a diluted Ising superlattice with a higher spin.

In this paper, we are concerned with the phase transitions and magnetic properties in a diluted spin-1 Ising superlattice consisting of two ferromagnetic materials with different bulk properties. For simplicity, we restrict our attention to the

case of simple cubic structures, but other structures can be treated without any difficulty. In particular, we consider the two constituents A and B with different bulk transition temperatures, i.e., $T_c^A \neq T_c^B$. The interface is, in general, different in nature from both bulks, even if the bulk critical temperatures are the same. We use the effective-field theory with a probability distribution technique[34] in the present work, as it is believed to be far superior to the standard mean-field approximation since it does not predict a zero critical concentration for diluted magnets. The method takes into consideration the fluctuations of the effective field and correctly accounts for all the single-site kinematic relations. The advantage of the probability distribution technique is that it allows the self-consistent equations that hold for an arbitrary lattice structure with a coordination number Z to be obtained and therefore results for different structures can be obtained without the detailed algebra encountered when employing other techniques. For the sake of simplicity, we assume that the concentration of magnetic atoms of the superlattice is homogenous.

Because of the periodicity of the superlattice structure, we restrict our discussions to a unit cell that interacts with its nearest-neighbor cells via the interface exchange interaction. Our major concerns are the dependence of the critical temperature on the interface exchange coupling, the influence of the concentration of magnetic atoms, and the interface exchange interaction on the critical temperature and the order parameters.

In the following section, we introduce the model and derive the equations that determine the layer longitudinal magnetizations, the quadrupolar moments, and the critical temperature. Numerical results are discussed in Sec. III. A brief conclusion is given in Sec. IV.

II. FORMALISM

We consider a superlattice consisting of two different ferromagnetic materials A and B stacked alternately: material A with L_a layers and material B with L_b layers. The exchange interaction between nearest-neighboring spins in $A(B)$ is denoted by $J_{aa}(J_{bb})$, while J_{ab} stands for the exchange interaction between the nearest-neighboring spins across the interface. The periodic condition suggests that we only have to consider one unit cell of the thickness $L=L_a+L_b$, which interacts with its nearest neighbors via the interface exchange interaction J_{ab}. The situation is depicted in Fig. 1. The Hamiltonian of the system is given by

$$H=-\sum_{(i,j)} J_{ij}c_i c_j S_{iz}S_{jz}, \tag{1}$$

where the sum runs over all nearest-neighbor spin pairs. S_{iz} denotes the z component of a quantum spin $\vec{S}_i$ of magnitude $S=1$ at site i, J_{ij} stands for one of the three exchange interactions depending on where the spin pair is located, and c_i is the occupation number on the lattice site i, $c_i=1$ if the lattice site is occupied by a magnetic atom and zero otherwise. The method we use is the effective-field theory[32–34] that employed the probability distribution technique to account for

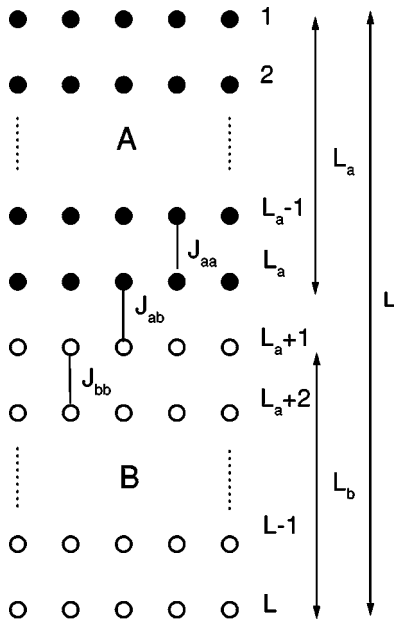

FIG. 1. Sketch of a unit cell of the superlattice.

the single-site spin correlations. Following that procedure, the layer longitudinal magnetization $\langle\langle c_i S_{iz}\rangle_c\rangle$ and the quadrupolar moment $\langle\langle c_i S_{iz}^2\rangle_c\rangle$ are given by

$$\begin{aligned} m_{iz}&=\langle\langle c_i S_{iz}\rangle_c\rangle=\langle c_i\langle S_{iz}\rangle_c\rangle=\langle c_i\rangle\langle\langle S_{iz}\rangle_c\rangle=c\langle\langle S_{iz}\rangle_c\rangle \\ &=c\left\langle \frac{2\sinh\left[\beta\left(\sum_j c_j J_{ij}S_{jz}\right)\right]}{1+2\cosh\left[\beta\left(\sum_j c_j J_{ij}S_{jz}\right)\right]}\right\rangle \\ &=c\left\langle f_{1z}\left(\sum_j c_j J_{ij}S_{jz}\right)\right\rangle \end{aligned} \tag{2}$$

$$\begin{aligned} q_{iz}&=\langle\langle c_i (S_{iz})^2\rangle_c\rangle=\langle c_i\rangle\langle\langle (S_{iz})^2\rangle_c\rangle=c\langle\langle (S_{iz})^2\rangle_c\rangle \\ &=c\left\langle \frac{2\cosh\left[\beta\left(\sum_j c_j J_{ij}S_{jz}\right)\right]}{1+2\cosh\left[\beta\left(\sum_j c_j J_{ij}S_{jz}\right)\right]}\right\rangle \\ &=c\left\langle f_{2z}\left(\sum_j c_j J_{ij}S_{jz}\right)\right\rangle, \end{aligned} \tag{3}$$

where m_{iz} and q_{iz} are, respectively, the longitudinal magnetization and quadrupolar order parameter of the ith site, $\beta=1/k_BT$, $\langle\cdots\rangle_c$ indicates the usual canonical ensemble thermal average for a given configuration, and the sum is over all the nearest neighbors of the site i, $\langle\cdots\rangle$ is the spatial configurational average. In a mean-field approximation, one would simply replace these spin operators by their thermal values m_z (the longitudinal magnetizations). However, it is at this point that a substantial improvement to the theory is made by noting that the spin operators have a finite set of base states, so that the averages over the functions f_{1z} and

f_{2z} can be expressed as an average over a finite polynomial of spin operators belonging to the neighboring spins. This procedure can be effected by the combinatorial method and correctly accounts for the single-site kinematic relations. Up to this point the theory is exact, but the right-hand sides of Eqs. (2) and (3) will contain multiple-spin-correlation functions. To perform spatial configurational averaging on the right-hand side of Eqs. (2) and (3), one now follows the general approach described in Refs. 32–34. Thus, with the use of the integral representation method of the δ Dirac's distribution, Eqs. (2) and (3) can be written in the form

$$m_{iz}=\int d\omega f_{1z}(\omega)\frac{1}{2\pi}\int dt\,\exp(i\omega t)\times\prod_j\langle\exp(-itc_jJ_{ij}S_{jz})\rangle, \tag{4}$$

$$q_{iz}=\int d\omega f_{2z}(\omega)\frac{1}{2\pi}\int dt\,\exp(i\omega t)\prod_j\langle\exp(-itc_jJ_{ij}S_{jz})\rangle, \tag{5}$$

where

$$f_{1z}(y)=\frac{2\sinh(\beta y)}{1+2\cosh(\beta y)}, \tag{6}$$

$$f_{2z}(y)=\frac{2\cosh(\beta y)}{1+2\cosh(\beta y)}, \tag{7}$$

and $\beta=1/K_bT$. In the derivation of the Eqs. (4) and (5), the commonly used approximation has been made according to which the multi-spin-correlation functions are decoupled into products of the spin averages.

To make progress, the simplest approximation of neglecting the correlations between different sites will be made. This is achieved by introducing the probability distribution of the spin variables S_{iz} given by[34]

$$P(c_i,S_{iz})=\frac{1}{3}(1-c)\delta(c_i)[\delta(S_{iz}+1)+\delta(S_{iz})+\delta(S_{iz}-1)]+\frac{1}{2}\delta(c_i-1)[(q_{iz}-m_{iz})\delta(S_{iz}+1)+2(c-q_{iz})\delta(S_{iz})+(q_{iz}+m_{iz})\delta(S_{iz}-1)], \tag{8}$$

with

$$c=\langle\langle c_i\rangle_c\rangle, \tag{9}$$

$$m_{iz}=\langle\langle c_iS_{iz}\rangle_c\rangle, \tag{10}$$

and

$$q_{iz}=\langle\langle c_iS_{iz}^2\rangle_c\rangle. \tag{11}$$

Allowing for the site magnetizations and quadrupolar moments to take different values in each atomic layer parallel to the surface of the superlattice, and labeling them in accordance with the layer number in which they are situated, the application of Eqs. (2), (4), and (8) yields the following set of equations for the layer longitudinal magnetizations:

$$\begin{aligned}m_{nz}=c2^{-N-2N_0}&\sum_{\mu=0}^{N}\sum_{\nu=0}^{N-\mu}\sum_{\mu_1=0}^{N_0}\sum_{\nu_1=0}^{N_0-\mu_1}\sum_{\mu_2=0}^{N_0}\sum_{\nu_2=0}^{N_0-\mu_2}2^{\mu+\mu_1+\mu_2}\\&\times C_\mu^N C_\nu^{N-\mu}C_{\mu_1}^{N_0}C_{\nu_1}^{N_0-\mu_1}C_{\mu_2}^{N_0}C_{\nu_2}^{N_0-\mu_2}(1-2q_{nz})^\mu\\&\times(q_{nz}-m_{nz})^\nu(q_{nz}+m_{nz})^{N-\mu-\nu}(1-2q_{n-1,z})^{\mu_1}\\&\times(q_{n-1,z}-m_{n-1,z})^{\nu_1}(q_{n-1,z}+m_{n-1,z})^{N_0-\mu_1-\nu_1}\\&\times(1-2q_{n+1,z})^{\mu_2}(q_{n+1,z}-m_{n+1,z})^{\nu_2}\\&\times(q_{n+1,z}+m_{n+1,z})^{N_0-\mu_2-\nu_2}f_{1z}([J_{n,n}(N-\mu-2\nu)\\&+J_{n,n-1}(N_0-\mu_1-\nu_1)+J_{n,n+1}(N_0-\mu_2-\nu_2)]),\end{aligned} \tag{12}$$

where N and N_0 are the numbers of nearest neighbors in the plane and between adjacent planes, respectively ($N=4$ and $N_0=1$ in the case of a simple cubic lattice with a coordination number $Z=N+2N_0$ that is considered here) and C_k^l are the binomial coefficients, $C_k^l=l!/k!(l-k)!$.

The equations of the longitudinal quadrupolar moments are obtained by substituting the function f_{1z} by f_{2z} in the expressions of the layer longitudinal magnetizations; this yields

$$q_{nz}=m_{nz}[f_{1z}(y)\rightarrow f_{2z}(y)]. \tag{13}$$

In this work we are interested in the calculation of the ordering near the transition critical temperature. The usual argument that m_{nz} tends to zero as the temperature approaches its critical value allows us to consider only terms linear in m_{nz} because higher-order terms tend to zero faster than m_{nz} on

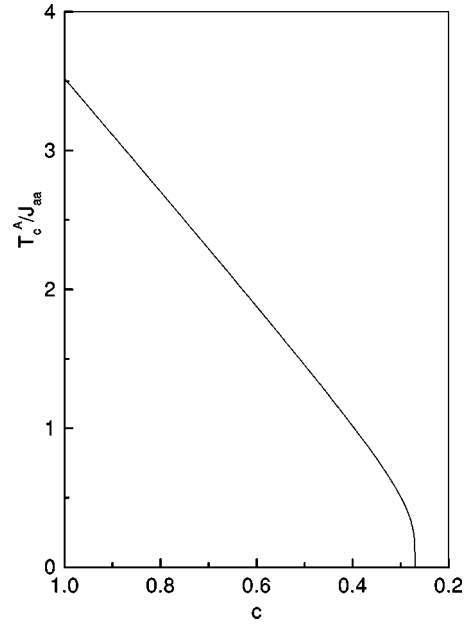

FIG. 2. Dependence of the critical temperature T_c^A/J_{aa} of an infinite bulk simple cubic lattice of material A on the concentration c of magnetic atoms.

approaching a critical temperature. Consequently, all terms of the order higher than linear terms in Eqs. (12) that give the expressions of m_{nz} can be neglected. This leads to the set of simultaneous equations

$$m_{nz}=A_{n,n-1}m_{n-1,z}+A_{n,n}m_{nz}+A_{n,n+1}m_{n+1,z}. \quad (14)$$

The system of Eqs. (14) is of the form

$$M\mathbf{m}_z=0, \quad (15)$$

where $\mathbf{m}_z$ is a vector of components $(m_{1z},m_{2z},\ldots,m_{nz},\ldots,m_{Lz})$ and the matrix M is symmetric and tridiagonal with elements

$$M_{i,j}=(A_{i,i}-1)\,\delta_{i,j}+A_{i,j}(\delta_{i,j-1}+\delta_{i,j+1}). \quad (16)$$

The only nonzero elements of the matrix M are given by

$$M_{n,n-1}=c2^{-N-2N_0}\sum_{\mu=0}^{N}\sum_{\nu=0}^{N-\mu}\sum_{\mu_1=0}^{N_0}\sum_{\nu_1=0}^{N_0-\mu_1}\sum_{\mu_2=0}^{N_0}\sum_{\nu_2=0}^{N_0-\mu_2}\sum_{i=0}^{\nu_1}\sum_{j=0}^{N_0-(\mu_1+\nu_1)}(-1)^i2^{\mu+\mu_1+\mu_2}\delta_{1,i+j}$$
$$\times C_\mu^N C_\nu^{N-\mu}C_{\mu_1}^{N_0}C_{\nu_1}^{N_0-\mu_1}C_{\mu_2}^{N_0}C_{\nu_2}^{N_0-\mu_2}C_i^{\nu_1}C_j^{N_0-(\mu_1+\nu_1)}(1-r_n)^\mu(1-r_{n-1})^{\mu_1}$$
$$\times(1-r_{n+1})^{\mu_2}r_n^{N-\mu}r_{n-1}^{(N_0-\mu_1)-(i+j)}r_{n+1}^{N_0-\mu_2}f_{1z}(y_n), \quad (17)$$

$$M_{n,n}=c\,2^{-N-2N_0}\sum_{\mu=0}^{N}\sum_{\nu=0}^{N-\mu}\sum_{\mu_1=0}^{N_0}\sum_{\nu_1=0}^{N_0-\mu_1}\sum_{\mu_2=0}^{N_0}\sum_{\nu_2=0}^{N_0-\mu_2}\sum_{i=0}^{\nu}\sum_{j=0}^{N-(\mu+\nu)}(-1)^i2^{\mu+\mu_1+\mu_2}\delta_{1,i+j}$$
$$\times C_\mu^N C_\nu^{N-\mu}C_{\mu_1}^{N_0}C_{\nu_1}^{N_0-\mu_1}C_{\mu_2}^{N_0}C_{\nu_2}^{N_0-\mu_2}C_i^{\nu}C_j^{N-(\mu+\nu)}(1-r_n)^\mu(1-r_{n-1})^{\mu_1}(1-r_{n+1})^{\mu_2}$$
$$\times r_n^{(N-\mu)-(i+j)}r_{n-1}^{N_0-\mu_1}r_{n+1}^{N_0-\mu_2}f_{1z}(y_n)-1, \quad (18)$$

$$M_{n,n+1}=c2^{-N-2N_0}\sum_{\mu=0}^{N}\sum_{\nu=0}^{N-\mu}\sum_{\mu_1=0}^{N_0}\sum_{\nu_1=0}^{N_0-\mu_1}\sum_{\mu_2=0}^{N_0}\sum_{\nu_2=0}^{N_0-\mu_2}\sum_{i=0}^{\nu_2}\sum_{j=0}^{N_0-(\mu_2+\nu_2)}(-1)^i2^{\mu+\mu_1+\mu_2}\delta_{1,i+j}$$
$$\times C_\mu^N C_\nu^{N-\mu}C_{\mu_1}^{N_0}C_{\nu_1}^{N_0-\mu_1}C_{\mu_2}^{N_0}C_{\nu_2}^{N_0-\mu_2}C_i^{\nu_2}C_j^{N_0-(\mu_2+\nu_2)}(1-r_n)^\mu(1-r_{n-1})^{\mu_1}$$
$$\times(1-r_{n+1})^{\mu_2}r_n^{N-\mu}r_{n-1}^{N_0-\mu_1}r_{n+1}^{(N_0-\mu_2)-(i+j)}f_{1z}(y_n), \quad (19)$$

where

$$y_n=J_{n,n}(N-\mu-2\nu)+J_{n,n-1}(N_0-\mu_1-\nu_1)+J_{n,n+1}(N_0-\mu_2-\nu_2) \quad (20)$$

and

$$r_n=c\,2^{-N-2N_0}\sum_{\mu=0}^{N}\sum_{\nu=0}^{N-\mu}\sum_{\mu_1=0}^{N_0}\sum_{\nu_1=0}^{N_0-\mu_1}\sum_{\mu_2=0}^{N_0}\sum_{\nu_2=0}^{N_0-\mu_2}2^{\mu+\mu_1+\mu_2}C_\mu^N C_\nu^{N-\mu}C_{\mu_1}^{N_0}C_{\nu_1}^{N_0-\mu_1}C_{\mu_2}^{N_0}C_{\nu_2}^{N_0-\mu_2}(1-2r_n)^\mu$$
$$\times r_n^{N-\mu}(1-2r_{n-1})^{\mu_1}r_{n-1}^{N_0-\mu_1}(1-2r_{n+1})^{\mu_2}r_{n+1}^{N_0-\mu_2}f_{2z}(y_n). \quad (21)$$

All the information about the critical temperature of the system is contained in Eq. (15). Up to now we did not precise the values of the exchange interactions; the terms in matrix (15) are general ones. In a general case, for arbitrary exchange interactions and the thickness of the superlattice the evaluation of the critical temperature relies on the numerical solution of the system of linear equations (15). These equations are fulfilled if and only if

$$\det M=0. \quad (22)$$

III. RESULTS AND DISCUSSION

In this paper, we take J_{aa} as the unit of energy, the length is measured in units of the lattice constant, and we introduce the reduced exchange interactions $R_1=J_{bb}/J_{aa}$ and $R_2=J_{ab}/J_{aa}$. Let us begin with the evaluation of the critical temperature with an example: the critical temperature of the site-diluted spin-1 Ising model for the simplest possible ''bulk case'' of a material A (i.e., $N=4,N_0=1,J_{i,j}=J_{aa}$). Then we can reduce $\det M$ to the following form:

$$\det M_{bulk}=\begin{vmatrix} a & b & & & & & & & & & b \\ b & a & b & & & & & & & & \\ & b & a & b & & & & & & & \\ & & & \cdots & \cdots & & & & & & \\ & & & & & b & a & b & & & \\ & & & & & & \cdots & \cdots & & & \\ & & & & & & & & b & a & b \\ & & & & & & & & & b & a \\ b & & & & & & & & & & \end{vmatrix}_{(L,L)}, \tag{23}$$

where the elements in the above determinant are given by

$$a=M_{n,n}(J_{n,n}=J_{n,n-1}=J_{n,n+1}=J_{aa}), \tag{24}$$

$$b=\frac{1}{4}(a+1), \tag{25}$$

and L in the ''bulk'' case is an arbitrary number. Now, we obtain the critical temperature from the condition $\det M_{bulk}=0$. This yields for $c=1$ to $T_c^A/J_{aa}=3.5186$, which is to be compared with the mean-field approximation result $T_c^A/J_{aa}=6$.

In Fig. 2, we show the behavior of the bulk critical temperature T_c^A/J_{aa} of the bulk material A as function of the concentration c of magnetic atoms. With the decrease of c, the phase region in which the ferromagnetic ordering is realizable gradually becomes small and vanishes at the bulk critical concentration $c_B=0.2706$ at which the bulk critical temperature T_c^A/J_{aa} reduces to zero.

A. Phase diagrams

In this section, we are interested in the study of the critical temperatures for the diluted ferromagnet spin-1 Ising superlattice. We remember that the exchange interactions between the nearest-neighbor spins in slabs A and B and across the interface are different. These differences influence the form of $\det M$, which can be written as

$$\begin{vmatrix} M_{1,1} & M_{1,2} & & & & & & & & & M_{1,L} \\ \cdots & \cdots & \cdots & \cdots & \cdots & \cdots & \cdots & \cdots & \cdots & \cdots & \\ & & & M_{L_a,L_a-1} & M_{L_a,L_a} & M_{L_a,L_a+1} & & & & & \\ & & & & M_{L_a+1,L_a} & M_{L_a+1,L_a+1} & M_{L_a+1,L_a+2} & & & & \\ \cdots & \cdots & \cdots & \cdots & \cdots & \cdots & \cdots & \cdots & \cdots & \cdots & \\ & & & & & & & M_{L-1,L-2} & M_{L-1,L-1} & M_{L-1,L} & \\ M_{L,1} & & & & & & & & M_{L,L-1} & M_{L,L} & \end{vmatrix}_{(L,L)}. \tag{26}$$

In order to calculate the critical temperatures of the superlattice, we have to solve Eq. (21) numerically in which we substitute $\det M$ by its expression given by Eq. (26).

Without loss of generality, we assume the critical temperature of slab A higher than that of slab B, that is, $J_{aa}\geqslant J_{bb}$ ($R_1=J_{bb}/J_{aa}\leqslant 1$), and hence $T_c^A/J_{aa}\geqslant T_c^B/J_{aa}$, where T_c^A/J_{aa} is the bulk critical temperature of a uniform lattice of material A and $T_c^B/J_{aa}=R_1T_c^A/J_{aa}$.

To study the effects of the reduced interface exchange $R_2=J_{ab}/J_{aa}$ and the concentration c of magnetic atoms on the critical temperature T_c/J_{aa} of the superlattice, T_c/J_{aa} is calculated as a function of R_2 for fixed $R_1=0.6$ and fixed $L_b=5$, but with various values of L_a and various values of the concentration c.

Figure 3(a) corresponds to the pure case $c=1$ and it shows that for $1\leqslant R_2\leqslant 7$, the dependence of the critical temperature T_c/J_{aa} on R_2 is approximately linear in agreement with the results of other methods.[10,13,14] For higher values of R_2, T_c/J_{aa} becomes nearly constant for each value of L_a. It is easy to see from this figure that there exists a critical value of the reduced interface exchange R_2^c such that, when $R_2>R_2^c$ and consequently $T_c/J_{aa}>T_c^A/J_{aa}, T_c^B/J_{aa}$, the system may order in the interface layers before it orders in the bulk, i.e., the interface magnetism dominates. For R_2 less than R_2^c, we have the contrary situation. The dashed horizontal line corresponds to the bulk critical temperature of material A for the concentration of magnetic atoms $c=1.0$.

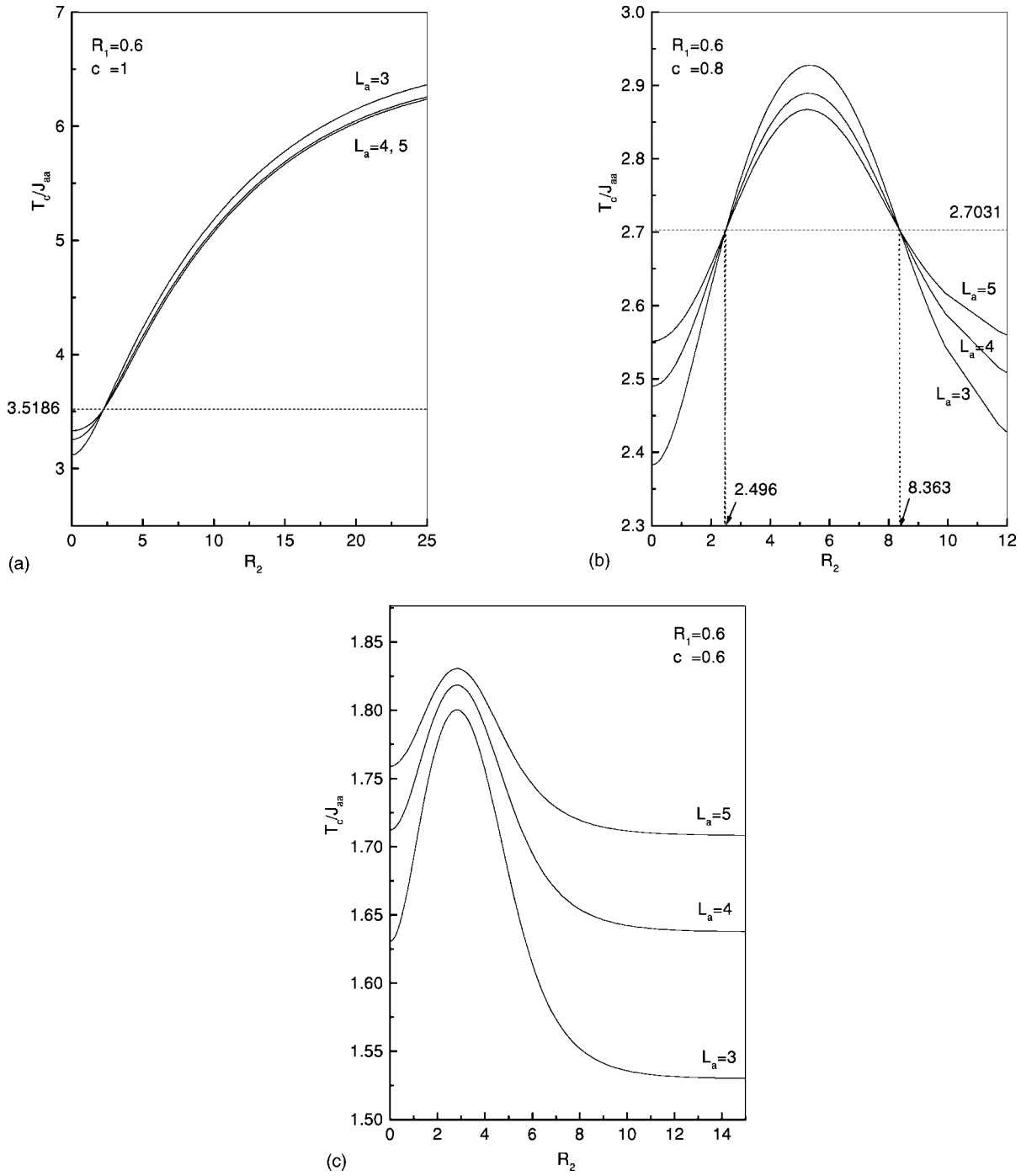

FIG. 3. (a) The critical temperature T_c/J_{aa} of the superlattice versus the reduced interface exchange interaction $R_2=J_{ab}/J_{aa}$ for $L_b=5$, $R_1=J_{bb}/J_{aa}=0.6$, and $c=1$. The number accompanying each curves denotes the value of L_a. (b) The critical temperature T_c/J_{aa} of the superlattice versus the reduced interface exchange interaction $R_2=J_{ab}/J_{aa}$ for $L_b=5$, $R_1=J_{bb}/J_{aa}=0.6$, and $c=0.8$. The number accompanying each curves denotes the value of L_a. (c) The critical temperature T_c/J_{aa} of the superlattice versus the reduced interface exchange interaction $R_2=J_{ab}/J_{aa}$ for $L_b=5$, $R_1=J_{bb}/J_{aa}=0.6$, and $c=0.6$. The number accompanying each curve denotes the value of L_a.

Figure 3(b) shows the dependence of T_c/J_{aa} on R_2 for the same values of the parameters as Fig. 3(a) ($L_b=5, R_1=0.6$), except here the concentration of magnetic atoms is $c=0.8$. The dashed horizontal line corresponds to the bulk critical temperature of material A for the concentration of magnetic atoms $c=0.8$. This figure exhibits some new interesting results for the diluted case. First, as is seen from this figure, the critical temperature curves show the reentrant phenomena; for a given value of T_c/J_{aa} there may exist two values of the interface exchange interaction R_2. This phenomena may be attributed to the competition between the effects of the exchange couplings and the dilution. Second, the dependence of T_c/J_{aa} on R_2 is completely different from the first case ($c=1$); it increases from a value that depends on L_a at R_2

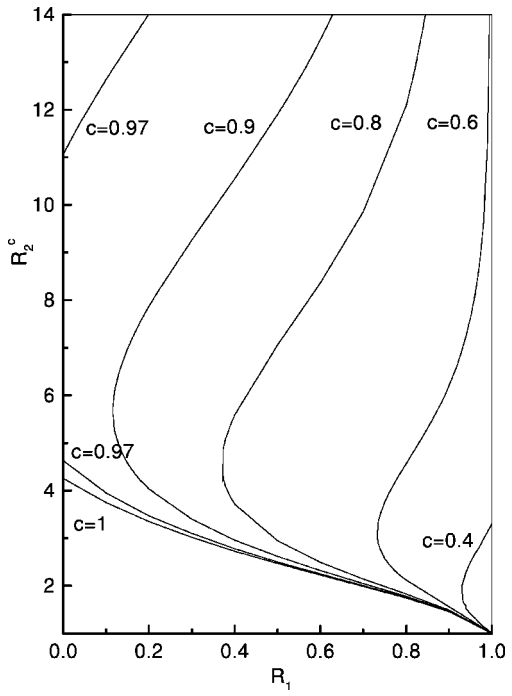

FIG. 4. Dependence of the reduced interface exchange coupling R_2^c on the reduced exchange coupling $R_1=J_{bb}/J_{aa}$ for $L_b=5$, and several values of the concentration c of magnetic atoms.

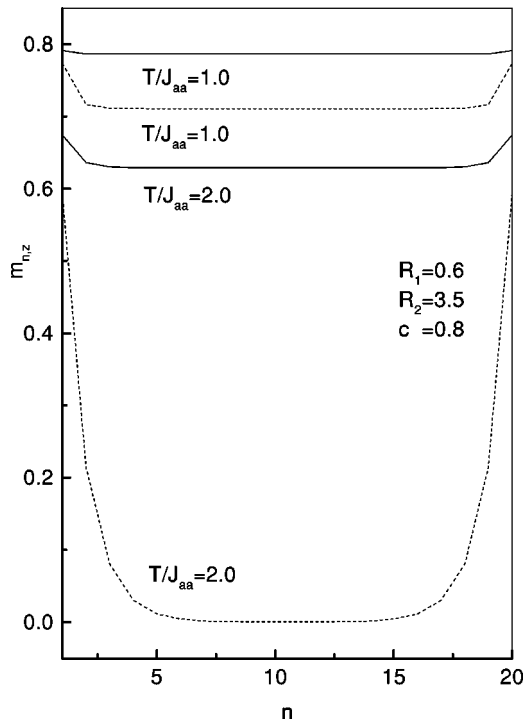

FIG. 5. Longitudinal magnetization profiles for a superlattice with $L=40$ layers when $R_1=J_{bb}/J_{aa}=0.6$, $R_2=J_{bb}/J_{aa}=3.5$, and $c=0.8$. The solid and dashed lines correspond respectively to the sublattice A and B. The number accompanying each curve denotes the value of temperature T/J_{aa}.

$=0$, passes through a maximum, and decreases for large values of R_2. Third, it is interesting to note that there exist two critical values of the reduced interface exchange $R_2^c:R_2^c=2.496$ and $R_2^c=8.363$, such that when $2.496<R_2<8.363$, and consequently $T_c/J_{aa}>T_c^A/J_{aa}, T_c^B/J_{aa}$, the system may order in the interface layer before it orders in the bulk; and when $R_2<2.496$ or $R_2>8.363$ we have the contrary situation.

Figure 3(c) shows the dependence of T_c/J_{aa} on R_2 for the same values of the parameters as Fig. 3(a) ($L_b=5, R_1=0.6$), except here the concentration of magnetic atoms is $c=0.6$. The variation of T_c/J_{aa} versus R_2 is the same as in Fig. 3(b), except that T_c/J_{aa} increases from a value that depends on L_a, at $R_2=0$, and it increases with the increase of L_a for L_b fixed. We note that the interface magnetism disappears in this case.

In Fig. 4, we show the phase diagram of the system by plotting the critical reduced interface exchange interaction R_2^c as a function of R_1 for different values of c. For the pure case, $c=1$, there exists a single value of R_2^c for all the values of R_1 and it decreases with the increase of R_1. For the diluted case, $c\neq 1$, it is seen that we have a range of R_1, which depends on c, where we find two values of the reduced critical interface exchange interaction. Otherwise this critical value does not exist. All the curves meet at the point of abscissa $R_1=1$ and of ordinate $R_2=R_2^c=1$.

B. Order parameters

In this section, we are interested in the study of the layer ordering parameters of the magnetic superlattice described above. These quantities depend on the temperature, the concentration of magnetic atoms, the reduced exchange interactions, and the unit-cell thickness L. We can obtain the layer longitudinal magnetizations and quadrupolar moments from Eqs. (12) and (13) as functions of temperature. We consider a superlattice with $L=40$ layers where $L_a=L_b=20$.

Four types of phase diagrams (the longitudinal magnetization $m_{n,z}$ profiles) are found depending on the values of the reduced exchange interactions R_1, R_2, the temperature, and the concentration of magnetic atoms. These phase diagrams correspond to the four possibilities for the magnetizations:

$$[m_{1,z}^A \geqslant m_{2,z}^A \geqslant m_{3,z}^A \quad \text{and} \quad m_{1,z}^B \geqslant m_{2,z}^B \geqslant m_{3,z}^B] \quad \text{(type 1)},$$

$$[m_{1,z}^A \leqslant m_{2,z}^A \leqslant m_{3,z}^A \quad \text{and} \quad m_{1,z}^B \leqslant m_{2,z}^B \leqslant m_{3,z}^B] \quad \text{(type 2)},$$

$$[m_{1,z}^A \leqslant m_{2,z}^A \leqslant m_{3,z}^A \quad \text{and} \quad m_{1,z}^B \geqslant m_{2,z}^B \geqslant m_{3,z}^B] \quad \text{(type 3)},$$

$$[m_{1,z}^A \geqslant m_{2,z}^A \geqslant m_{3,z}^A \quad \text{and} \quad m_{1,z}^B \leqslant m_{2,z}^B \leqslant m_{3,z}^B] \quad \text{(type 4)}.$$

These diagrams are shown respectively in Figs. 5–8 for some selected values of the reduced exchange interactions R_1, R_2, c, and T/J_{aa}. The solid and dotted curves correspond to the magnetization profile of the sublattice A and B, respectively. The number accompanying each curve denotes the value of the temperature T/J_{aa}. Because of the symmetry of the superlattice, we limit the interpretation to the first half of the layers. The variation of longitudinal quadrupolar moments $q_{n,z}$ versus n is the same as $m_{n,z}$ versus n.

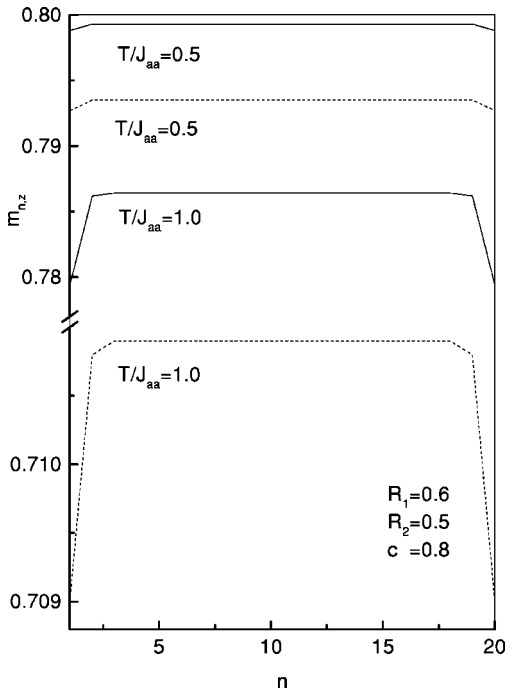

FIG. 6. Longitudinal magnetization profiles for a superlattice with $L=40$ layers when $R_1=J_{bb}/J_{aa}=0.6$, $R_2=J_{bb}/J_{aa}=0.5$, and $c=0.8$. The solid and dashed lines correspond respectively to the sublattice *A* and *B*. The number accompanying each curve denotes the value of temperature T/J_{aa}.

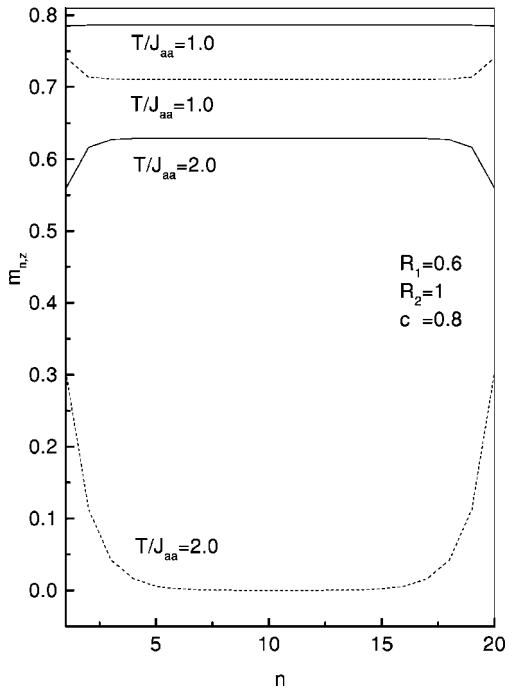

FIG. 7. Longitudinal magnetization profiles for a superlattice with $L=40$ layers when $R_1=J_{bb}/J_{aa}=0.6$, $R_2=J_{bb}/J_{aa}=1.0$, and $c=0.8$. The solid and dashed lines correspond respectively to the sublattice *A* and *B*. The number accompanying each curve denotes the value of temperature T/J_{aa}.

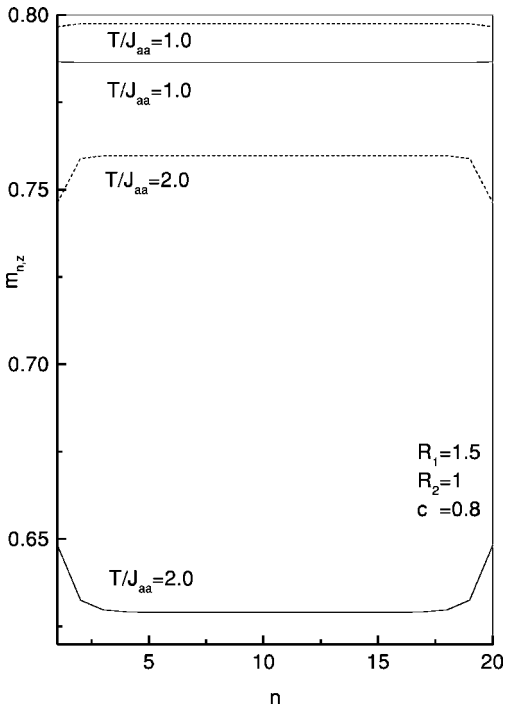

FIG. 8. Longitudinal magnetization profiles for a superlattice with $L=40$ layers when $R_1=J_{bb}/J_{aa}=1.5$, $R_2=J_{bb}/J_{aa}=1.0$, and $c=0.8$. The solid and dashed lines correspond respectively to the sublattice *A* and *B*. The number accompanying each curve denotes the value of temperature T/J_{aa}.

We present the magnetization profiles in Fig. 5 for $R_1=0.6$, $R_2=3.5$, $c=0.8$, and two values of the temperature: $T/J_{aa}=1.0$, and $T/J_{aa}=2.0$. We see that the longitudinal magnetizations $m_{n,z}$ have their largest values at the interfaces and they decrease with the number of layers to reach their minimal values in the bulk ($n=10$). This suggests that there exists an interface magnetism in the system. It is interesting to note that the effect of the interface is more significant at high temperature; $m_{n,z}$ decrease with the increase of the temperature T/J_{aa} as expected.

We present the magnetization profiles in Fig. 6 for $R_1=0.6$, $R_2=0.5$, $c=0.8$, and two values of the temperature: $T/J_{aa}=0.5$, and $T/J_{aa}=1.0$. We see that the longitudinal magnetizations $m_{n,z}$ have their smallest values at the interfaces and they increase with the number of layers to reach their maximal values in the bulk ($n=10$). It is interesting to note that there is no interface magnetism in this case; $m_{n,z}$ decrease with the increase of the temperature T/J_{aa} as expected.

In Figs. 7 and 8 we show the magnetization profiles for $R_2=1.0$, $c=0.8$, and two values of the temperature: $T/J_{aa}=1.0$ and $T/J_{aa}=2.0$ and for $R_1=0.6$ and $R_1=1.5$, respectively. In these cases we can see that the interface magnetism is only present in one sublattice, in sublattice *B* for the first case and in the sublattice *A* in the second case.

IV. CONCLUSION

In conclusion, we have studied the critical behavior and some magnetic properties of the diluted spin-1 Ising model

of magnetic superlattice consisting of two materials, using the effective-field theory with a probability distribution technique that accounts for the self-spin correlation function.

For the pure case, a critical value R_2^c of the reduced interlayer exchange interaction R_2 has been found such that for $R_2 > R_2^c$ the interface magnetism dominates, and for $R_2 < R_2^c$ we have the contrary situation.

As discussed in Sec. III A, the study of the effect of the dilution on the critical temperature of the system is very significant: The behavior of the system is different from the pure case ($c=1$). A number of interesting phenomena have been found such as the reentrant behavior in the critical temperature curves that can be attributed to the competition between the exchange couplings and the dilution. We can also see that depending on R_1 and c, the system may exhibit two critical values of the reduced interface coupling. It is interesting to note that the interface magnetism does not exist for every values of c and R_1.

We have also studied the magnetizations (and the quadrupolar moments) versus the number of layers of the unit cell and have shown that these phase diagrams exhibit four types depending on R_1, R_2, c, and T/J_{aa}. This study also shows the existence of the interface magnetism in the system.

The formalism of transition temperature derivation obtained above is general and can be used for the study of superlattices of various thicknesses and structures. Although we have discussed only ferromagnetic exchanges (all $J>0$), the formulation is applicable to antiferromagnetic couplings as well.

ACKNOWLEDGMENTS

This work was done during a visit of M.S. and M.K. to the Université de Metz, France in the frame of the Action integrée No. 46/SM/97.

[1] R.E. Camley and R.L. Stamps, J. Phys.: Condens. Matter **5**, 3727 (1993).
[2] M.A. Thompson and J.L. Erskine, Phys. Rev. B **31**, 6832 (1985).
[3] M.E. Onellion, C.L. Fu, M.A. Thompson, J.L. Erskine, and A.J. Freeman, Phys. Rev. B **33**, 7322 (1986).
[4] M. Farle and K. Baberschke, Phys. Rev. Lett. **58**, 511 (1987).
[5] W. Durr, M. Taborelli, O. Paul, R. Germar, W. Gudat, D. Pescia, and M. Landotlt, Phys. Rev. Lett. **62**, 206 (1989).
[6] L.L. Hinchey and D.L. Mills, Phys. Rev. B **33**, 3329 (1986).
[7] L.L. Hinchey and D.L. Mills, Phys. Rev. B **34**, 1689 (1986).
[8] F. Fishman, F. Schwable, and D. Schwenk, Phys. Lett. A **121**, 192 (1987).
[9] R.E. Camley and D.R. Tilley, Phys. Rev. B **37**, 3413 (1988).
[10] D.R. Tilley, Solid State Commun. **65**, 657 (1988).
[11] J. Barnaś, J. Phys. C **21**, 1021 (1988).
[12] J. Barnaś, J. Phys.: Condens. Matter **2**, 7173 (1990).
[13] H.K. Sy and M.H. Ow, J. Phys.: Condens. Matter **4**, 5891 (1992)
[14] H.K. Sy, Phys. Rev. B **45**, 4454 (1992).
[15] A. Saber, I. Essaoudi, A. Ainane, and M. Saber, Phys. Status Solidi B **209**, 161 (1998).
[16] L.J. de Jongh and A.R. Miedema, Adv. Phys. **23**, 1 (1974).
[17] T.E. Wood and P. Day, J. Phys. C **10**, L333 (1977) .
[18] P. Wong and P.M. Horn, Bull. Am. Phys. Soc. **24**, 363 (1979).
[19] S. Oscroff, R. Calvo, and W. Giriat, J. Appl. Phys. **50**, 7738 (1979).
[20] T. Shinjo, N. Hosoito, K. Kawaguchi, T. Takada, Y. Endoh, Y. Ajiro, and J.M. Friedt, J. Phys. Soc. Jpn. **52**, 3154 (1983).
[21] C. Rau, C. Jin, and M. Robert, J. Appl. Phys. **63**, 3667 (1988).
[22] T. Kaneyoshi, I. Tamura, and E.F. Sarmento, Phys. Rev. B **28**, 6491 (1983).
[23] Qiang Hong, Phys. Rev. B **41**, 9621 (1990).
[24] Qiang Hong, Phys. Rev. B **44**, 10 101 (1991).
[25] A. Benyoussef, N. Boccara, and M. Saber, J. Phys.: Condens. Matter **18**, 4275 (1985).
[26] A.R. Ferchmin and W. Maciejewski, J. Phys.: Condens. Matter **12**, 4311 (1979).
[27] A. Saber, A. Ainane, M. Saber, I. Essaoudi, F. Dujardin, and B. Stébé, Phys. Rev. B **6**, 4149 (1999).
[28] J.W. Tucker, J. Magn. Magn. Mater. **102**, 144 (1991).
[29] Z.Y. Li, S.L. Xu, D.L. Lin, and T.F. George, Physica B **182**, 249 (1992).
[30] J.L. Zhong, C.Z. Yang, and J.L. Li, J. Phys.: Condens. Matter **3**, 1301 (1991).
[31] Cheng Jia and Xuan-Zhang Wang, J. Phys.: Condens. Matter **8**, 5745 (1996).
[32] A. Saber, A. Ainane, F. Dujardin, N. El Aouad, M. Saber, and B. Stébé, J. Phys.: Condens. Matter **12**, 43 (2000).
[33] A. Saber, A. Ainane, F. Dujardin, M. Saber, and B. Stébé, J. Phys.: Condens. Matter **11**, 2087 (1999).
[34] J.W. Tucker, M. Saber, and L. Peliti, Physica A **206**, 497 (1994).